Numerical Assessment of the Experimental Thermoelectric Cooling System Effectiveness

Justyna Gołębiowska[1*], Marcin K. Widomski[1]

[1] Faculty of Environmental Engineering, Lublin University of Technology, ul. Nadbystrzycka 40B, 20-618 Lublin, Poland

* Corresponding author's e-mail: j.golebiowska@pollub.pl

ABSTRACT

Solid-state thermoelectric elements, such as thermoelectric (TE) modules, can be used as cooling devices. Small-sized TE modules, characterized by: lack of moving parts, no required refrigerants application as well as variable possible installation and operation positions, allow, in several specified cases, achieving the advantage in cooling process over the conventional refrigeration devices. This paper presents the results of the preliminary numerical determination of energetic efficiency of thermoelectric cooling system, applied for cooling a small-scale experimental room. The heat exchangers used in the cooling system consisted of heat sinks and radiators installed on the both sides of the TE module. The numerical assessment included in this paper, based on a 3D model reflecting the experimental room and thermoelectric cooling system, allowed determining the relation between TE module power supply characteristics and cooling effects, as well as time-related temperature distribution inside the modeled experimental room. The commercial modeling software FLUENT, ANSYS 12.0 by ANSYS Inc. was applied in numerical calculations. The results of the performed laboratory studies were used as a basis for model development, required input data, initial and boundary conditions. The results of laboratory tests showed the influence of amperage of power supply on the efficiency of cooling characteristics, as well as distribution of air temperature inside the experimental room. Calibration and validation of the developed model was also based on the results of laboratory experiment. The obtained results of numerical calculations showed the influence of amperage of power supply on efficiency of cooling characteristics as well as distribution of air temperature inside the experimental room.

Keywords: COP, numerical modeling, thermoelectric cooling, cooling effectiveness.

INTRODUCTION

Nowadays, nearly 20% of the total electricity used in the buildings is related to indoor cooling. The International Energy Agency warns that without any action addressed toward increasing the energy efficiency of cooling process, energy demand will triple by the middle of the 21st century [IEA 2018].The use of thermoelectric technology in buildings has been investigated intensely for the last two decades. In many scientific publications, cited later in this work, TE modules are presented as promising devices that can be incorporated to many system configurations to achieve indoor thermal comfort and reduction of primary energy consumption, especially from the non-renewable resources. Thermoelectric cooling (TEC) is based on the Peltier effect, which causes absorption or rejection of the heat when an electric current flows through the interface of two semiconductor elements: n-type (N) or p-type (P), due to the difference in thermal energy transferred by the charge carriers [Enescu and Virjoghe 2014, Sarbu and Dorca 2018]. Modern and commercialized TE modules are built mainly from bismuth telluride (Bi_2Te_3) (the information about different TE materials can be found in Selvan et al. [2019] and Soleimani et al. [2020]) and placed between two ceramic plates. The P-N or N-P junctions, forming a TE module, are connected electrically in series and thermally in parallel. The direction of the current flow determines which side is cold and which is hot [Twaha et al. 2016]. Schematic construction of the TE module is presented in Figure 1.

The cooling capacity of the cold side of the TE module can be calculated from the following equation [Enescu and Virjoghe 2014]:

$$Q_c = \alpha I T_c - K\Delta T - \frac{1}{2}R_e I^2 \qquad (1)$$

where: α is Seebeck coefficient [V/K], I – input current [A], T_c – temperature of cold junction [K], K – thermal conductance of the thermoelements in parallel [W/K], ΔT – temperature difference between hot and cold sides [K], $R_e I^2$ – is a Joule heat [W] depending on the electrical resistance [Ω] of the thermoelement and input power [A].

More information connected with modeling of TE modules can be found in Enescu and Virjoghe [2014], Lineykin and Ben-Yaakov [2007], Zhao and Tan [2014] or Żelazna and Gołębiowska [2020]. Thermoelectric modules can be also used as electric current generators (TEG) when an opposite phenomenon described by Seebeck effect occurs, i.e. when a temperature difference is achieved on both sides of the TE module [Zoui et al. 2020, Alahmer et al. 2022].

Typical applications of TE modules include cooling of electronic devices, cold generation in refrigeration (primarily mobile devices used mainly in cars or for touristic purposes) as well as precision temperature control in laboratory and medical equipment [He et al. 2015, Jangonda et al. 2016, Sarbu and Dorca 2018]. More innovative applications of TE modules may refer to cooling of photovoltaic (PV) panels [Kane et al. 2017, Dimri et al. 2018], temperature-control vehicle seats [Elarusi et al. 2017, Su et al. 2018] or even thermoregulatory garment [Zhao et al. 2018, Lou et al. 2020]. Owing to a compact size, fast reaction, elimination of moving parts and refrigerants application, opportunity to work also in heating mode and variable possible operation positions, TE modules can be successfully used as cooling devices and support the control of the personal thermal comfort parameters. In Fig. 2, four examples of TE implementation were presented. In the recent years, many scientific articles describing the use of TE modules to influence the indoor air temperature in buildings have been published in order to verify if they can be an alternative to more complex compressor chillers (despite the lower performance efficiency). For instance, two first cases refer to the TE modules used in active building envelopes. In Xu et al. [2007], an active building window (ABW) was presented in order to provide both, cooling and heating (Fig. 2c). In the long time tests, in the cooling mode, it was possible to reduce and maintain the temperature of the TE modules cold sides 5°C below the ambient temperature. In the heating mode, the temperature of the hot sides of TE modules was 40°C above the ambient temperature.

In Wang et al. [2021], a simple structure of the integral thermoelectric building wall (ITEW) was proposed and investigated. The authors prepared large-scale thermoelectric plates that can be used as building walls. Optimization showed that COP in the cooling mode ranged from 2 to 7 and the cooling capacity per unit area can range from 2 to 70 W/m². Liu et al. [2015] presented the theoretical and experimental research on a thermoelectric solar air conditioner with the possibility of heat recovery for heating domestic water. The proposed system was investigated in three operating modes: space cooling, space cooling and heat recovery for water heating, space heating. The experiments showed that air cooling and water heating mode was characterized by relatively high COP coefficient, reaching slightly above 4.5.
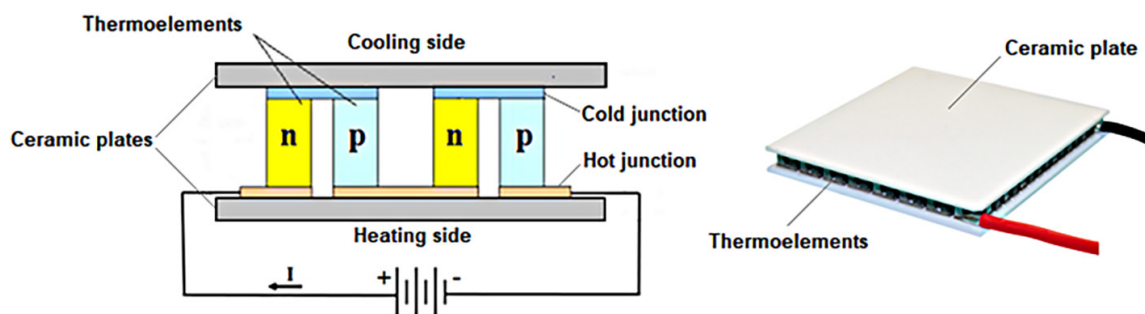

Figure 1. Schematic construction of TE module (on the left) and commercial TE module (on the right) (based on Enescu and Virjoghe [2014])
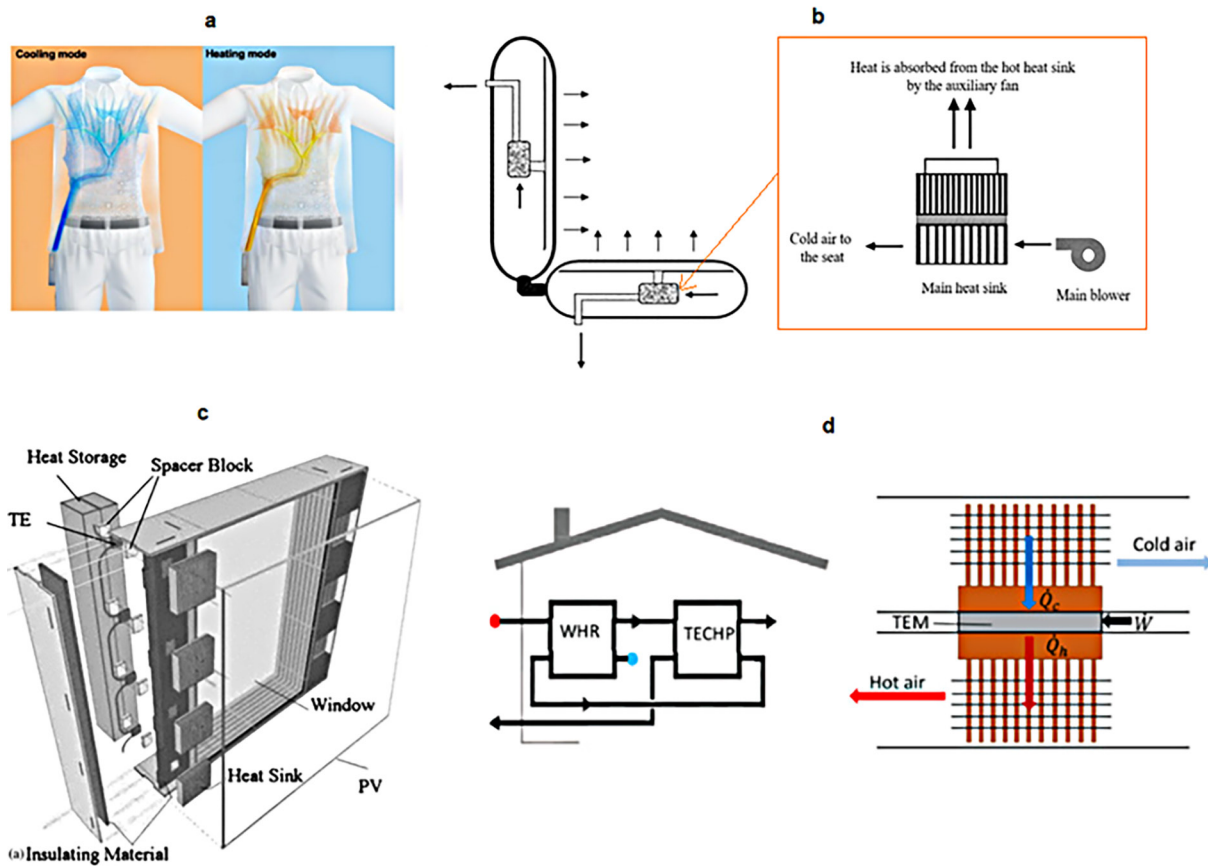
Figure 2. Examples of the TE modules application: a) thermoelectric air conditioning undergarment [Lou et al. 2020]; b) thermoelectric cooling/heating system for car seat climate control [Elarusi et al. 2017]; c) active building window system [Xu et al. 2007]; d) thermoelectric cooler-heat pump [Arangure et al. 2019]

An experimental and simulation investigation of a thermoelectric air duct system (TE-AD) for space cooling under tropical weather conditions was described in Irshad et al. [2017]. In the presented case, TE-AD was supported by the photovoltaic (PV) system. The conducted experiments showed that, owing to this novel solution, 517 W of cooling capacity was provided to the test room and COP at level 1.15 was achieved. The authors estimated that in the particular case study, proposed system (combination of the TE-AD and PV system) could save 1806.75 kWh/year.

Another example, presented in Arangure et al. [2019], referred to a thermoelectric cooler-heat pump (TECHP) supported by heat pipes used as a heat exchangers (Fig. 2d). Together with waste heat recovery unit, TECHP was a part of a mechanical ventilation system applied into nearly zero energy building (nZEB). In the experimental results COP of TE cooler varied from 0.46 up to 5.25, depending on the cooling heat fluxes, mass flows and the position of the modules. As it may be observed based on the cited literature, TE modules can be applied in many different systems configurations supporting the cooling process. However, the application of the TE modules to a specific system should be additionally tested by fluid flow models to assess the effectiveness of the air and temperature distribution as the performance of the TE module is highly effected by the type of heat exchanger applied to support the heat transfer from the TE module ceramic surfaces [Liu et al. 2015, Afshari 2022] or even the geometry of the heat sink [Yilmazoglu 2016, Seo et al. 2018].

The purpose of the research presented in this paper was to numerically determine the efficiency of thermoelectric cooling system, consisting of heat sinks and radiators installed on the both sides of the TE module, installed in a small-scale experimental room. The performed numerical simulations, based on 3D model reflecting the experimental room and thermoelectric cooling system, allowed assessing the relation between TE module power supply characteristics and cooling effects as well as time-related temperature distribution inside the modeled experimental room.

MATERIALS AND METHODS

The 3D multivariate numerical modeling of thermoelectric cooling system efficiency presented in this paper was directly based on the laboratory measurements enabling to obtain the input data as well as the initial and boundary conations for numerical modeling and calibration of the developed three dimensional model. The laboratory tests were conducted using a laboratory set based on a small scale polystyrene chamber of internal cubature 0.125 m³, see Fig. 3. Thermal conductivity coefficient of the implemented Styrofoam material obtained from the available technical documentation, provided by the producer, was 0.034 W/(m·K) and the thickness of experimental chamber walls was 5 cm. The thermoelectric module QC-127-1.4-8.5MD by QUICK-COOL (Germany) was used in the experiment. The TE module was installed in movable cover of the chamber (the cover was also an insulation of the TE module). The tested module was applied to decrease the air temperature inside the experimental chamber. The heat generated on the hot side of the module was treated as a waste heat. On the both sides of the applied TE module, heat exchangers were installed: two sets of aluminum heat sinks with adjusted fans. Heat exchangers were crucial to improve the heat transfer between the two sides of the TE module, whereas fans improved the heat dissipation inside the chamber and waste heat dissipation to the surroundings.

The calibrated measurement and recording system was applied in order to measure the air temperature inside the chamber as well as temperature on the cold and hot side of the TE module. The measuring system consisted of six Pt 500 temperature sensors (measuring accuracy ± 0.1 K) connected to the data recorder. The thermoelectric module was powered by direct current (from laboratory power supply) of amperage equaled to 4 A, 5 A, 6 A and 7 A. One measurement series lasted 90 minutes. The temperature values in all points were measured every minute. Measuring series for one value of applied current were repeated three times.

Numerical calculations of heat transfer and temperature distribution inside the air experimental room, cooled by the tested TE module, were performed in the commercial finite elements modeling software FLUENT, ANSYS 12.0 by ANSYS Inc. The developed preliminary model, consisted of 70094 nodes and 345986 finite elements, reflected experimental room of volume 0.125 m³, radiator and fan. The developed geometry reflecting the real object of modeled domain is presented in Figure 4a while finite elements mesh, after discretization of the geometry,
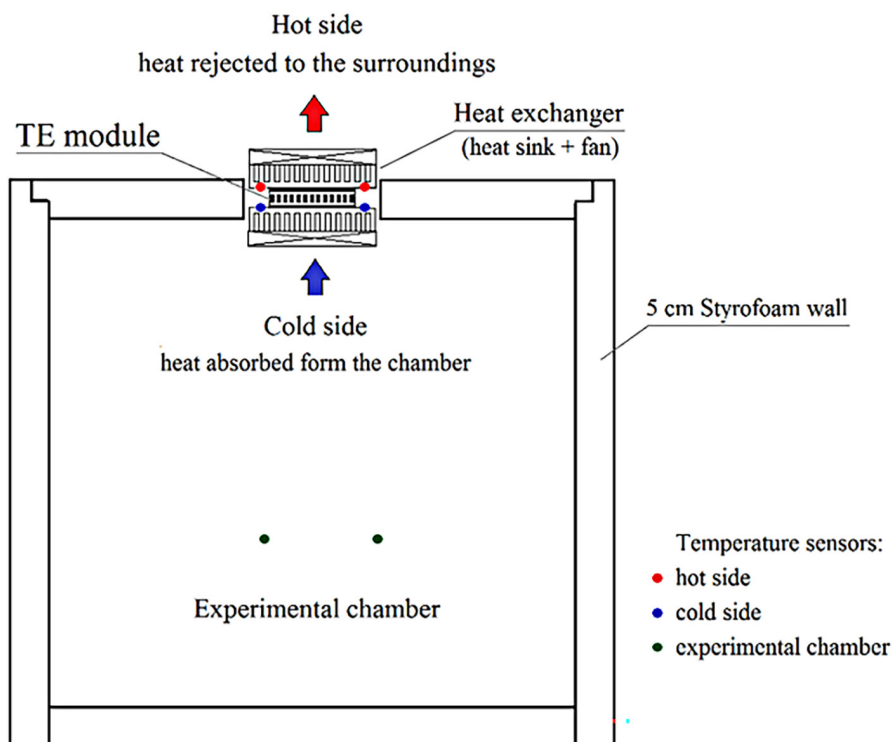

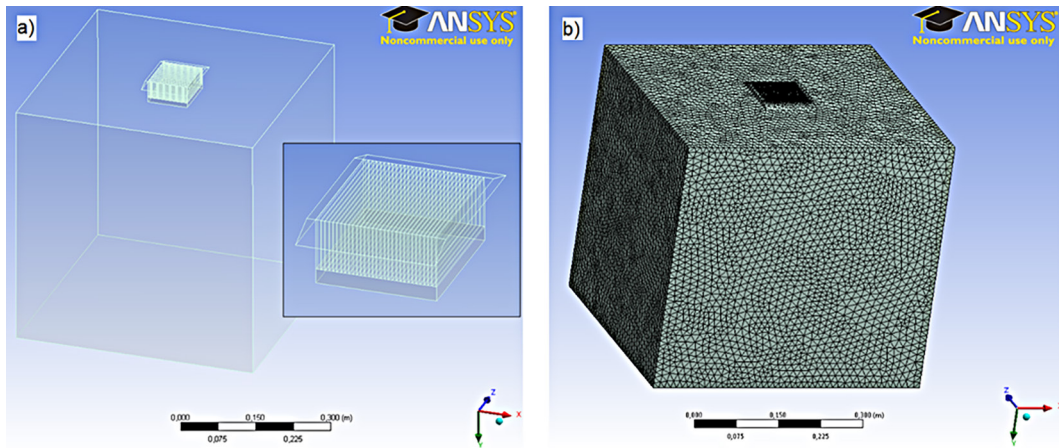**Figure 3.** Scheme of laboratory experimental chamber

Figure 4. Numerical model assumed for modeling: a) modeled geometry; b) finite volumes mesh

is shown in Figure 4b. The model contained the simplified solution for fan modeling. The small finite volume was distinguished above the radiator and the constant value of air velocity, measured directly in the laboratory experimental room by air speed meter model number 435-2 by Testo AG (Germany), equal to 2.53 m/s was assigned to the whole volume of this part. The realizable k-epsilon model of viscous air turbulent flow supported with energy transfer equation was used in the employed model [Comini and Del Giudice 1985]. Time duration of simulation was equal to time of experiment, i.e. 90 minutes.

Numerical calculations were performed for four values of amperage supplying the TE module: 4 A, 5 A, 6 A and 7 A. The required input data covered air and aluminum characteristics, including density, specific heat, thermal conductivity

and dynamic viscosity, assumed for preliminary model as based on three point linear characteristics. The assumed input data as well as initial conditions for air inside the experimental chamber are presented in Table 1.

The following characteristics of aluminum were assigned to the radiator zone: density 2719 kg/m^3, specific heat 871 J/(kg·K) and thermal conductivity 202.4 W/(m·K). The assumed initial conditions covered the value of air temperature assigned to the air zone (see Table 1). There were two simplified types of boundary conditions assigned to the adopted model. The first one, the variable, time-related wall temperature in the radiator zone reflected outflow of heat from the modeled domain. The second, time-related wall heat transfer, calculated, using Eq. 2, for determined difference of temperature inside and

Table 1. Input data assumed for numerical modeling

Current	Initial air temperature	Temperature: at the beginning, after 10 min., at the end	Air density	Specific heat	Dynamic viscosity	Thermal conductivity coeff.
[A]	[K]/[°C]	[K]/[°C]	[kg/m^3]	[J/(kg·K)]	[kg/(m·s)]	[W/(m·K)]
4	293.65/20.5	293.65/20.5	1.203	1006.1	$1.82 \cdot 10^{-5}$	0.025633
		290.15/17	1.217	1006.0	$1.81 \cdot 10^{-5}$	0.02537
		284.15/11	1.243	1005.8	$1.78 \cdot 10^{-5}$	0.024916
5	293.15/20	293,15/20	1.205	1006.1	$1.82 \cdot 10^{-5}$	0.025596
		288.45/15.3	1.224	1005.9	$1.80 \cdot 10^{-5}$	0.025242
		284.05/10.9	1.244	1005.8	$1.78 \cdot 10^{-5}$	0.024908
6	293.25/20.1	293.25/20.1	1.204	1006.1	$1.82 \cdot 10^{-5}$	0.025603
		289.65/16.5	1.219	1006	$1.80 \cdot 10^{-5}$	0.025332
		286.55/13.4	1.233	1005.9	$1.79 \cdot 10^{-5}$	0.025098
7	293.55/20.4	293.55/20.4	1.203	1006.1	$1.82 \cdot 10^{-5}$	0.02562
		291.35/18.2	1.212	1006.0	$1.81 \cdot 10^{-5}$	0.02546
		291.45/18.3	1.212	1006.0	$1.81 \cdot 10^{-5}$	0.02547

outside the experimental room, area of the wall and thickness (5 cm) as well as thermal conductivity of Styrofoam (0.034 W/(mK)). Both mentioned boundary conditions were determined for two periods, initial, with the duration of approx. 5 minutes, and remaining, the rest of experiment time duration. This partition was related to the temperature changes of radiator and air inside the chamber observed under laboratory conditions. The possible additional heat transfer through joints of Styrofoam plates was not included in the adopted model.

$$q_H = \lambda \frac{T_e - T_i}{l} \qquad (2)$$

where: q_H – a heat flux [W ·m²], λ – a thermal conductivity [W/(m·K)], T_e – an exterior temperature [K], T_i – an interior temperature [K], l – a wall thickness [m].

The boundary conditions assigned to each variant of computation are presented in Table 2. The amount of the heat absorbed from the closed environment, e.g. an interior of experimental chamber, can be calculated from [Afshari 2022]:

$$Q_c = m \cdot C_\rho \cdot \Delta T - Q_{loss} \qquad (3)$$

where: m – a air mass in closed space [kg], C_ρ – a specific heat capacity ([J/(kg·K)], ΔT – a temperature difference of the cooled air inside the experimental chamber [K], Q_{loss} – a heat loss through the wall during the experiment [Wh].

Table 2. Range of boundary conditions values assumed for numerical modeling

Current value	Radiator zone temperature	Wall heat flux
[A]	[K]/[°C]	[W/m²]
4	289.69 - 285.25/16.54-12.1	0.187 - 6.120
5	288.70 - 281.45/15.55-8.3	0.734 - 2.958
6	290.22 - 284.45/17.07-11.3	0.381 - 2.120
7	290.56 - 290.15/17.41-17.00	0.165 - 1.150

Coefficient of the performance (COP) of the tested system can be calculated from the following equation [Afshari 2022]:

$$COP = \frac{Q_c}{E_{TE} + E_{Fan}} \qquad (4)$$

where: Qc – an energy absorbed from the chamber (descireb in eq. 3) [Wh], E_{TE} – an energy consumed by the TE module [Wh], E_{fan} – an energy consumed by the fans [Wh].

RESULTS

The time-related changes of temperature difference between cold and hot side of the TE module (ΔT) observed under laboratory conditions, directly affecting Qc, as well as the measured temperature of air inside the experimental room are presented in Figure 5. The results of temperature measurements presented in Figure 5 show the direct
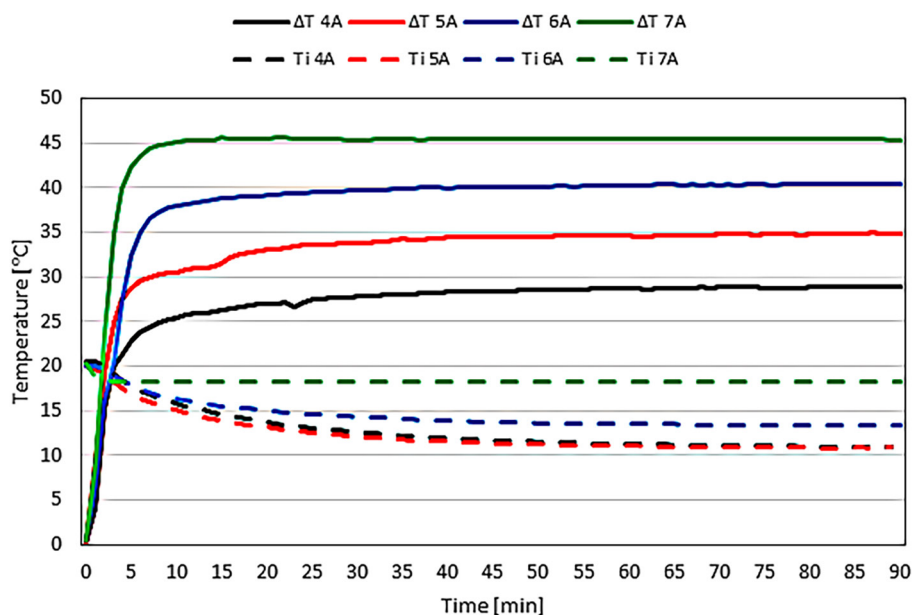

Figure 5. Experimental results of measurements: air temperature inside the experimental room (T_i) and the temperature difference between cold and hot side of the TE module (ΔT)

relation between the current amperage applied to power the tested TE module and obtained temperature values in monitored points. The higher the value of applied current, the greater the difference between temperatures on the cold and hot sides of TE module as well as the lower decrease in air temperature inside the experimental chamber were observed. Thus, the increase in current amperage triggers changes in cooling capacity or the total heat transfer rate of TE module, directly affected by the observed difference between measured temperatures of module cold and hot side. The increased temperature on the hot side, related to the increased amperage, in case of insufficient heat exchanger application, results in decreased cooling efficiency, reflected by the elevated air temperature inside the experimental room. The above-mentioned phenomenon is directly related to the changes in Peltier's and Joule's heat as well as heat transfer of TE module.

Figure 6 shows the comparisons of two determined values: Q_c – heat absorbed form the chamber during the experiments according to Eq. 3 as well the total energy consumed by the cooling system calculated as a sum of: E_{TE} – energy consumed by the TE module and E_{fan} – energy consumend by the fans in the heat exchangers. Again, according to the data presented in Fig. 6, the value of current amperage applied to power the studied TE module directly affects its cooling efficiency. The best cooling results, understood as Qc, were

noted for the lowest applied current amperage i.e. 4 A and 5 A. For higher current values, a decrease in cooling system efficiency was observed. In contrast, the energy consumption by the system increases significantly with the increase in the amperage applied to the TE. It is connected with the energy delivered to the TE module as the energy consumed by the fans was the same for all tested series (approx. 8 Wh].

The achieved *COP* values (taking values from 0.01 to 0.14) are presented in Figure 7 and were calculated according to Eq. 4. The best results were achieved for the appied current value of 4 A and equaled 0.14. For the higher values of the cuurrent applied to the module, the decrease in the cooling performance can be observed, which is a result of the additional heat generated inside the module (Joule's heat) as well as the heat conduction of the heat form the hot side of TE module to the cold side of the module that was already mentioned in this work. The achieved values of *COP* are simmilar to ones presented in the literature for the simmilar systems [Afshari 2022].

Figures 8-11 show the distributions of modeled air temperature and velocity magnitude inside the experimental chamber for selected time steps of simulation duration achieved due to implementation of the Fluent software. The observed air velocity distributions are comparable in all studied cases. In contrast, the determined time related air temperature values and spatial distribution vary
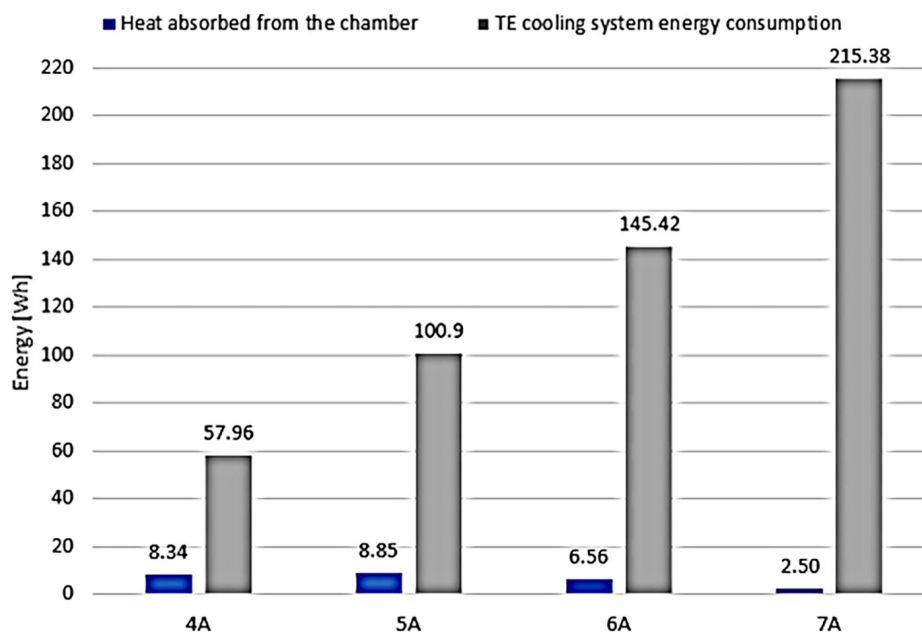

Figure 6. Heat absorbed from the chamber during the experiment (Q_c) and energy delivered to power TE cooling system ($E_{TE} + E_{fan}$)
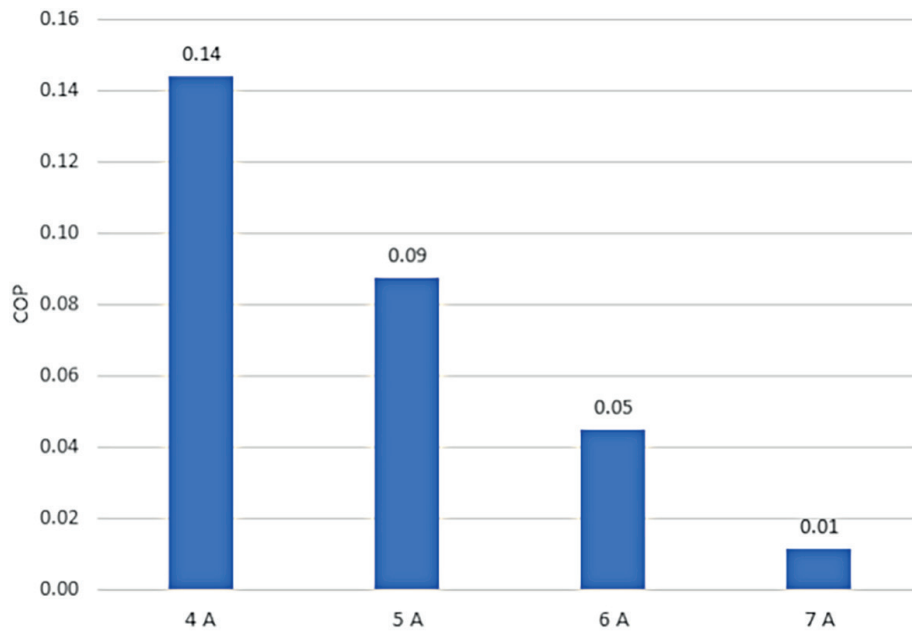
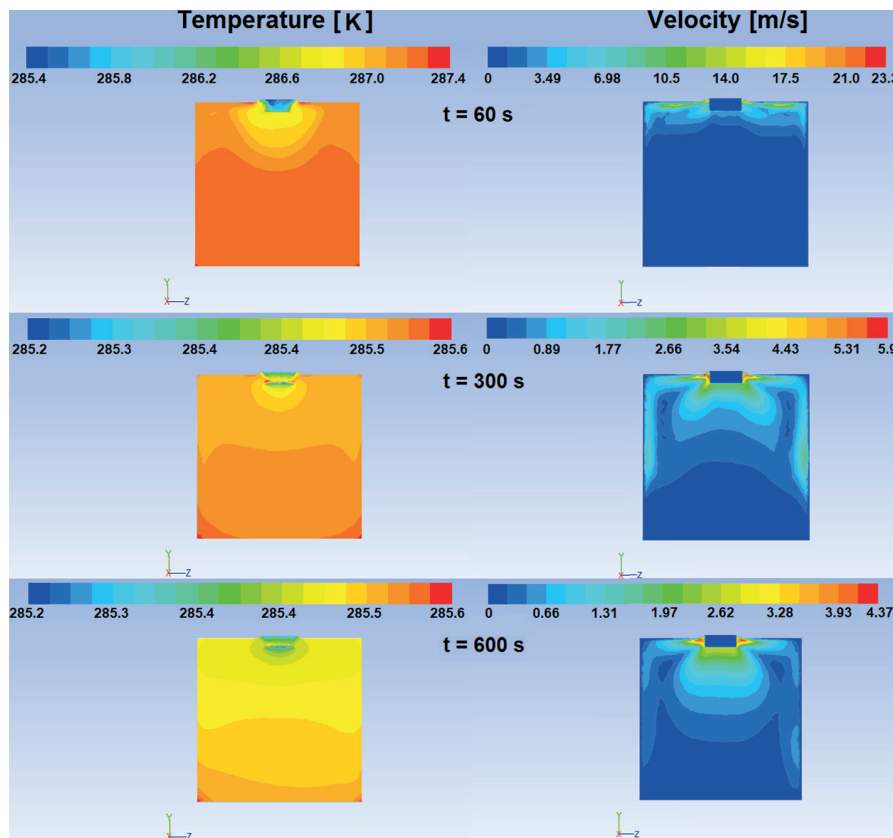**Figure 7.** Coefficient of the performance obtained during the experiments

Figure 8. Results of modeling for different amperage values 4 A and various time steps, including air temperature and velocity distributions

depending on the applied current value. The highest ratio of modeled internal temperature values drops were noted for the lowest applied current value. In Table 3, the comparison of measured and modeled values of final internal air temperature, obtained for different amperage is presented. The difference between the obtained results for different compared series varies from 0.37 to 0.76%, in
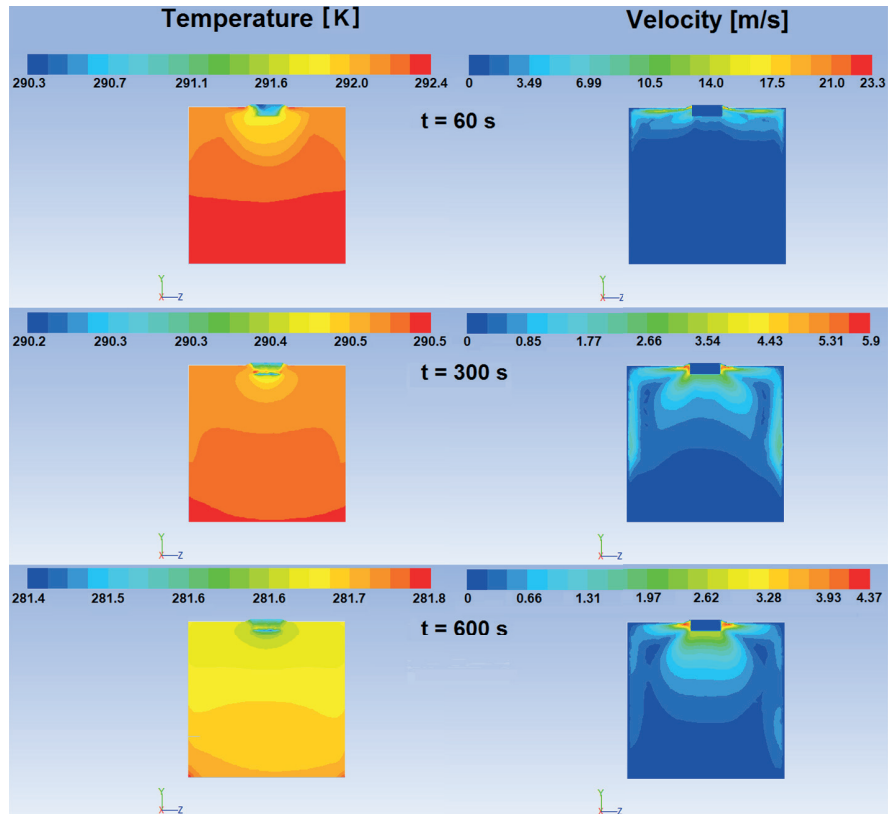
Figure 9. Results of modeling for different amperage values 5 A and various time steps, including air temperature and velocity distributions
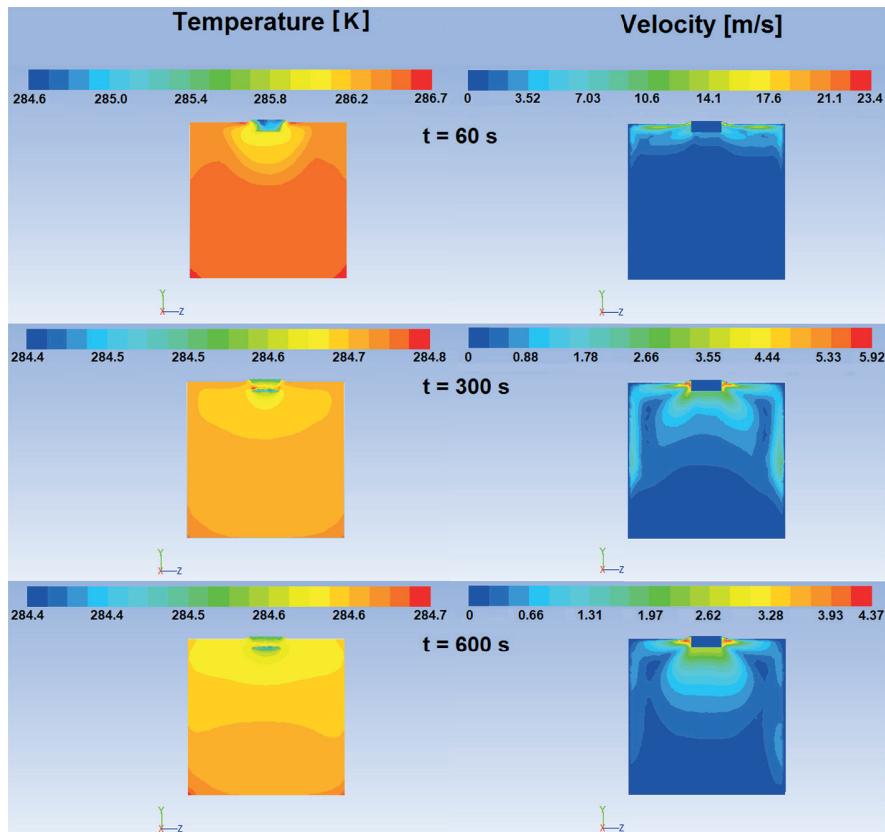

Figure 10. Results of modeling for different amperage values 6 A and various time steps, including air temperature and velocity distributions
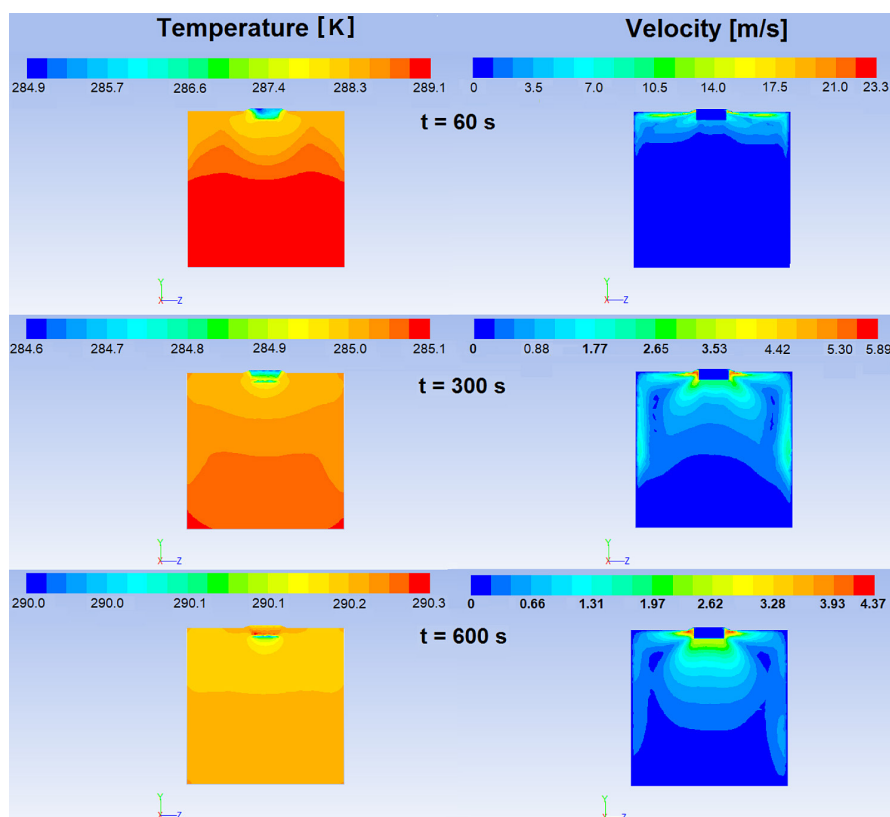
Figure 11. Results of modeling for different amperage values 7 A and various time steps, including air temperature and velocity distributions

Table 3. The final internal air temperature according to the measurements and modeling results

Current value	Measured final air temperature	Modeled final air temperature	The percentage difference between obtained results
[A]	[K]/[°C]	[K]/[°C]	[%]
4	284.15/11	282.82/9.67	0.47
5	284.03/10.88	281.88/8.73	0.76
6	286.52/13.37	285.19/12.04	0.46
7	291.47/18.32	290.40/17.25	0.37

Table 4. The results of the numerical model validation including R, R^2 and RSME

Current value	R	R^2	RSME
[A]	[-]	[-]	[K]
4	0.826	0.682	3.285
5	0.857	0.734	3.136
6	0.817	0.667	2.217
7	0.990	0.980	1.026

favor of the measured values. Thus, the calculated final temperature values appeared to be slightly underestimated. Table 4 shows the results of numerical model validation by determined values of R, R^2 and RSME for comparison of measured and calculated air temperature for the whole duration of experiment with frequency equal to one minute. The calculated RSME values vary between approx. 1.0 and 3.3 K. The determined correlation and determination coefficient, R and R^2, values show strong positive correlations between the measured and calculated air temperature values, all determined R values were greater than 0.7.

CONCLUSIONS

In this paper, the assessments of a thermoelectric cooling system operation as well as its effectiveness numerical determination were performed.

On the basis of the conducted experimental and computational analysis, the following conclusions can be drawn. The general relation between power characteristics and effective cooling energy rate, affected by the TE module total heat transfer rate and heat of thermal conduction from outside environment, was observed. Generally, increase in the value of current supplying the tested TE module equipped in the particular heat exchanger reduces its cooling efficiency reflected by relatively low decrease in air temperature inside the cooled room and significant increase in measured temperature on the hot side of the module.

The observed cooling effect depends directly on the current applied to the TE module. The best cooling results were achieved for the 4 A current, for which the temperature inside the experimental room decreased from 20.5 to 11°C. For this series, the efficiency of the system was also the highest – COP = 0.14. In general, application of TE module and the proposed heat exchanger allowed decreasing temperature inside the experimental room by 2.1–9.5°C. The heat obtained on the hot side (treated in this experiment as a waste heat), reflected by high values of the temperature determined on the hot side of TE module, can be reused for a certain purpose such as preliminary heating of domestic water. Thus, the overall system efficiency can be improved. The applied method of numerical modeling allowed successful assessment of time-related changes in velocity of flow and temperature distribution of air inside the experimental chamber.

Numerical calculations showed a relation between current amperage and local air temperature changes inside the experimental room. The highest decrease in temperature drop was related to decrease in the applied amperage value of TE module power supply. In all modeled variants, distribution of air velocity inside the modeled room was comparable, because it was closely related to fan efficiency, which was assumed the same for all studied cases.

REFERENCES

1. Afshari F. 2021. Experimental and numerical investigation on thermoelectric coolers for comparing air-to-water to air-to-air refrigerators. Journal of Thermal Analysis and Calorimetry, 144(3), 855–868.

2. Alahmer A., Khalid M.B., Beithou N., Borowski G., Alsaqoor S. and Alhendi H. 2022. An Experimental Investigation into Improving the Performance of Thermoelectric Generators. Journal of Ecological Engineering, 23(3), 100–108.

3. Aranguren P., DiazDeGarayo S., Martínez A. Araiz M. and Astrain D. 2019. Heat pipes thermal performance for a reversible thermoelectric cooler-heat pump for a nZEB. Energy and Buildings, 187, 163–172.

4. Comini G., Del Giudice S. 1985. A (k-epsilon) model of turbulent flow. Numerical Heat Transfer, 8(2), 133–147.

5. Dimri N., Tiwari A., Tiwari G.N. 2018. Effect of thermoelectric cooler (TEC) integrated at the base of opaque photovoltaic (PV) module to enhance an overall electrical efficiency. Solar Energy, 166, 159–170.

6. Elarusi A., Attar A. and Lee H. 2017. Optimal design of a thermoelectric cooling/heating system for car seat climate control (CSCC). Journal of Electronic Materials, 46(4), 1984–1995.

7. Enescu D., Virjoghe E.O. 2014. A review on thermoelectric cooling parameters and performance. Renewable and Sustainable Energy Reviews, 38, 903–916.

8. He W., Zhang G., Zhang X.X., Ji J., Li G.Q., Zhao X.D. Recent development and application of thermoelectric generator and cooler. Appl. Energy. 2015, 143, 1–25.

9. IEA, 2018: https://www.iea.org/reports/the-future-of-cooling

10. Irshad K., Habib K., Basrawi F., Saha B.B. 2017. Study of a thermoelectric air duct system assisted by photovoltaic wall for space cooling in tropical climate. Energy, 119, 504–522.

11. Jangonda C., Patil K., Kinikar A., Bhokare R. and Gavali M.D. 2016. Review of various application of thermoelectric module. International journal of innovative research in science, engineering and technology, 5(3), 3393–3400.

12. Kane A., Verma V., Singh B. 2017. Optimization of thermoelectric cooling technology for an active cooling of photovoltaic panel. Renewable and Sustainable Energy Reviews, 75, 1295–1305.

13. Lineykin S., Ben-Yaakov S. 2007. Modeling and analysis of thermoelectric modules. IEEE Transactions on Industry Applications, 43(2), 505–551.

14. Liu Z.B., Zhang L., Gong G., Luo Y., Meng F. 2015. Experimental study and performance analysis of a solar thermoelectric air conditioner with hot water supply. Energy and buildings, 86, 619–625.

15. Lou L., Shou D., Park H., Zhao D., Wu Y.S., Hui X., Yang R., Kan E.C. and Fan J. 2020. Thermoelectric air conditioning undergarment for personal thermal management and HVAC energy saving. Energy and Buildings, 226, 110374.

16. Mirmanto M., Syahrul S. and Wirdan Y. 2019. Experimental performances of a thermoelectric cooler box with thermoelectric position variations.

Engineering Science and Technology, an International Journal, 22(1), 177–184.

17. Sarbu I., Dorca,A. 2018. A comprehensive review of solar thermoelectric cooling systems. International Journal of Energy Research, 42(2), 395–415.

18. Selvan K.V., Hasan M.N. and Mohamed Ali M.S. 2019. State-of-the-art reviews and analyses of emerging research findings and achievements of thermoelectric materials over the past years. Journal of Electronic Materials, 48(2), 745–777.

19. Seo Y.M., Ha M.Y. Park S.H., Lee G.H., Kim Y.S. and Park Y.G. 2018. A numerical study on the performance of the thermoelectric module with different heat sink shapes. Applied Thermal Engineering, 128, 1082–1094.

20. Soleimani Z., Zoras S., Ceranic B., Shahzad S. and Cui Y. 2020. A review on recent developments of thermoelectric materials for room-temperature applications. Sustainable Energy Technologies and Assessments, 37, 100604.

21. Su C., Dong W., Deng Y., Wang Y., Liu X. 2018. Numerical and experimental investigation on the performance of a thermoelectric cooling automotive seat. Journal of Electronic Materials, 47(6), 3218–3229.

22. Twaha S., Zhu J., Yan Y., Li B. 2016. A comprehensive review of thermoelectric technology: Materials, applications, modelling and performance improvement. Renewable and Sustainable Energy Reviews, 65, 698–726.

23. Wang P., Liu Z., Chen D., Li W., Zhang L. 2021. Experimental study and multi-objective optimisation of a novel integral thermoelectric wall. Energy and Buildings, 252, 111403.

24. Xu X., Van Dessel S., Messac A. 2007. Study of the performance of thermoelectric modules for use in active building envelopes. Building and Environment, 42(3), 1489–1502.

25. Yilmazoglu M.Z. 2016. Experimental and numerical investigation of a prototype thermoelectric heating and cooling unit. Energy and Buildings, 113, 51–60.

26. Zhao D., Tan G. 2014. A review of thermoelectric cooling: materials, modeling and applications. Applied thermal engineering, 66(1–2), 15–24.

27. Zhao D., Lu X., Fan T., Wu Y.S., Lou L., Wang Q., Fan J., Yang R. 2018. Personal thermal management using portable thermoelectrics for potential building energy saving. Applied Energy, 218, 282–291.

28. Zoui M.A., Bentouba S., Stocholm J.G., Bourouis M. 2020. A review on thermoelectric generators: Progress and applications. Energies, 13(14), 3606.

29. Żelazna A., Gołębiowska J. 2020. A PV-Powered TE Cooling System with Heat Recovery: Energy Balance and Environmental Impact Indicators. Energies, 13(7), 1701.